

Copyright is owned by the Author of the thesis. Permission is given for a copy to be downloaded by an individual for the purpose of research and private study only. The thesis may not be reproduced elsewhere without the permission of the Author.

---

Crystallographic Determination of  
Wild Type, Mutant and Substrate-  
Analogue Inhibited Structures of  
Bacterial Members of a Family of  
Superoxide Dismutases

by

Simon Hardie Oakley

*Submitted as part of the requirements for the  
degree of*

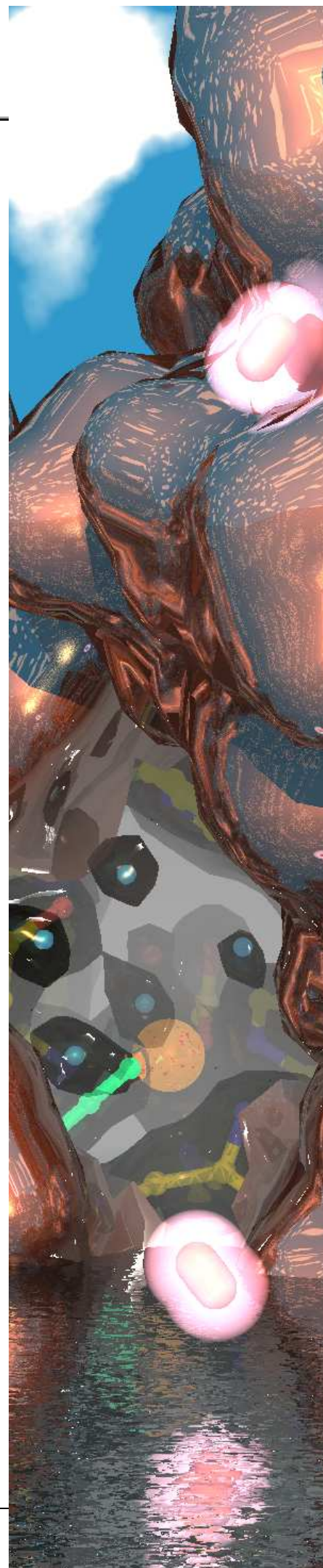
Doctor of Philosophy

Institute of Fundamental Sciences,  
Chemistry

Massey University, New Zealand

2009

---





"Part of the inhumanity of the computer is that, once it is competently programmed and working smoothly, it is completely honest."

Isaac Asimov (1920-92), author,  
inventor of the word "robotics".

## 0.1 Abstract

### **Crystallographic Determination of Wild Type, Mutant and Substrate-Analogue Inhibited Structures of Bacterial Members of a Family of Superoxide Dismutases**

The iron and manganese superoxide dismutases are a family of metallo-enzymes with highly conserved protein folds, active sites and dimer interfaces. They catalyse the elimination of the cytotoxic free radical superoxide to molecular oxygen and hydrogen peroxide by alternate reduction then oxidation of the active-site with the concomitant transfer of protons from the solvent. There are many key aspects of enzymatic function that lack a structural explanation.

The focus of this study is on three crystal structures. The iron-substituted manganese superoxide dismutase from *Escherichia coli* complexed with azide, a substrate-mimicking inhibitor, was solved to 2.2 Å. This “wrong” metal form shows a binding pattern seen previously in the manganese superoxide dismutase from *Thermus thermophilus*. Wild-type manganese specific superoxide dismutase from the extremophile *Deinococcus radiodurans* was solved to 2.0 Å and has an active site reminiscent of other solved manganese superoxide dismutases despite a lack of product inhibition. The azide-inhibited manganese superoxide dismutase from *Deinococcus radiodurans* was determined to a resolution of 2.0 Å and showed binding of azide, and by inference superoxide, different to that seen in *Thermus thermophilus*, but reminiscent of that seen in azide-inhibited iron superoxide dismutases. These results indicate that the azide ion, and by inference superoxide, bind to the metal centre of manganese superoxide dismutases in two modes, and transition between the two modes may be entropy dependent.

These structures, integrated with knowledge from other structures, known biochemistry and various spectra, provide insight into catalytic function. An outer-sphere mechanism of proton transfer that does not rely on through-peptide proton uptake is proposed and compared to a previously proposed inner-sphere mechanism. This is based on the observation that a water molecule moves into the active site of the manganese superoxide dismutase from *Deinococcus radiodurans* upon azide binding, providing a Grötthus pathway for rapid proton transfer to the active site from the bulk solvent.

Also presented in this study are the partially refined structures of four point mutants (S82T, L83M, L133V, and M164L/L166V) of the manganese superoxide dismutase from *Escherichia coli* all solved to roughly 2 Å resolution, designed to investigate product inhibition which varies across species.

---

## 0.2 Acknowledgements

Acknowledgement pages generally read like a mix between an Oscar acceptance speech and a shopping list, so here goes. There are many people who contributed to my time at Massey University both professionally and social. Therefore to quote the bard, “brevity is the sole of wit” I apologise to all those not named specifically in my efforts to be both laconic and pretentious.

Firstly, would like to acknowledge my supervisor Geoff for his support, encouragement and vast knowledge on all things chemical, X-ray, and crystal.

Secondly, the post-docs; my co supervisor Bryan for answering questions about various computer software and crystallography, and Jim, whose brief foray into protein crystallography from chemistry was very fruitful.

Thirdly, Gill, Trev, and the other members of the X-lab past and present for providing lab space, office space, computing, stolen pens, interesting talks, moral encouragement, cakes, parties, beer, wine, gossip *et cetera*. These were all gladly accepted but not always reciprocated.

Penultimately, I would like to thank my various flat-mates and friends over my time in Palmerston North who put up with my bad jokes and stories over the past few years.

Lastly, but most importantly, I would like to thank my family for their long-distance encouragement and support.

-Simon

<b>0.3</b>	<b>Table of contents</b>	
<b>0.1</b>	<b>Abstract</b>	<b>iii</b>
<b>0.2</b>	<b>Acknowledgements</b>	<b>iv</b>
<b>0.3</b>	<b>Table of contents</b>	<b>v</b>
<b>0.4</b>	<b>List of figures</b>	<b>xiii</b>
<b>0.5</b>	<b>List of equations</b>	<b>xix</b>
<b>0.6</b>	<b>List of tables</b>	<b>xxi</b>
<b>0.7</b>	<b>Abbreviations</b>	<b>xxii</b>
<b>0.8</b>	<b>Naming conventions of superoxide dismutases</b>	<b>xxv</b>
<b>1</b>	<b>The prehistory and history of the superoxide dismutase protein families</b>	<b>1</b>
<b>1.1</b>	<b>Background on oxygen, oxygen toxicity and identification of superoxide</b>	<b>1</b>
<b>1.2</b>	<b>Early biochemistry and structures</b>	<b>2</b>
<b>1.3</b>	<b>Roles of superoxide and SODs</b>	<b>6</b>
<b>1.4</b>	<b>Medical importance</b>	<b>6</b>
<b>1.5</b>	<b>Catalytic turnover, catalytically perfect enzymes</b>	<b>7</b>
<b>1.6</b>	<b>Prevalent theories as to how enzymes promote catalysis</b>	<b>8</b>
<b>1.7</b>	<b>Evolution of SODs</b>	<b>9</b>
1.7.1	Extinct SODs	10
1.7.2	Direct evolution	11
1.7.3	Horizontal transfer	11
1.7.4	Recent radiation	12
1.7.5	Multiple SODs	12
1.7.6	Transferring information between SOD families	12
1.7.7	Differences in SOD expression	13
1.7.8	Post-transcriptional control of SODs	13
<b>1.8</b>	<b>Oligomers</b>	<b>13</b>
<b>1.9</b>	<b>Convergent evolution with convergent mechanism</b>	<b>14</b>

<b>2</b>	<b>The Fe/MnSOD family .....</b>	<b>19</b>
2.1	Genomic era.....	19
2.2	Macromolecular structure and contribution to active-site architecture.....	20
2.3	Dimer interface.....	20
2.4	Differences in quaternary structure .....	22
2.5	Solvent-access funnel to the Fe/MnSODs .....	25
2.6	Fe/MnSOD knowledge derived from spectroscopy, structures and biochemistry.....	27
2.7	Second shell and third shell of residues .....	28
2.8	Wrong metal forms.....	28
2.9	Metal specificity amongst Fe/MnSODs.....	29
2.10	Metal specificity as a method of control.....	30
2.11	Serious alterations to hydrogen-bonding networks.....	31
2.12	Tyrosine of the solvent-access funnel.....	33
2.13	Product inhibition in MnSODs.....	34
2.14	Differences in inhibition by small-molecule inhibitors.....	35
2.15	SODs with very low affinity for azide.....	36
2.16	General trends amongst FeSODs compared to MnSODs.....	37
2.17	Current hypotheses for differences between FeSODs and MnSODs.....	37
2.18	Tuning redox potential .....	38
2.19	pH dependences are different between the FeSODs and the MnSODs.....	38
2.20	Metal-substituted Fe/MnSODs with altered p <i>K</i> .....	43
2.21	Unresolved issues in the structure and function of the Fe/MnSOD family.....	43

<b>2.22</b>	<b>Scope of this thesis.....</b>	<b>45</b>
<b>2.23</b>	<b>Why research was undertaken .....</b>	<b>46</b>
2.23.1	An iron-substituted form of a manganese-specific SOD inhibited by azide a substrate mimic .....	47
2.23.2	An MnSOD from an extremophile .....	47
2.23.3	An azide-inhibited MnSOD solved at cryogenic conditions .....	48
<b>3</b>	<b>Methods.....</b>	<b>49</b>
<b>3.1</b>	<b>Methods used to solve and refine the azide-inhibited iron-substituted MnSOD from <i>E. coli</i> .....</b>	<b>49</b>
3.1.1	Crystallisation .....	49
3.1.2	Data collection, merging and molecular replacement .....	49
3.1.3	Refinement.....	50
<b>3.2</b>	<b>Methods used to solve MnSOD from the extremophile <i>Deinococcus radiodurans</i>.....</b>	<b>52</b>
3.2.1	Crystallisation and crystal mounting.....	52
3.2.2	Data collection .....	53
3.2.3	Molecular replacement and initial maps .....	54
<b>3.3</b>	<b>Methods used to solve the azide-inhibited MnSOD from <i>Deinococcus radiodurans</i>.....</b>	<b>55</b>
3.3.1	Crystallisation and mounting .....	55
3.3.2	Data collection, reduction and merging .....	56
3.3.3	Molecular replacement and initial maps .....	56
<b>3.4</b>	<b>Attempted high-temperature data collection .....</b>	<b>57</b>
3.4.1	220 K data collection.....	57
3.4.2	Room temperature data collection .....	58
<b>3.5</b>	<b>Structures of four <i>Ec</i>-MnSOD mutants.....</b>	<b>58</b>
3.5.1	Materials .....	58
3.5.1.1	General .....	58
3.5.1.2	Enzymes .....	58
3.5.1.3	Crystallisation supplies and mounting equipment.....	59
3.5.2	Mutation.....	59
3.5.3	Expression.....	62
3.5.4	Isolation by ammonium sulfate cut.....	62
3.5.5	Low pressure chromatography .....	63
3.5.5.1	Cation exchange chromatography .....	63
3.5.5.2	Anion exchange chromatography .....	64
3.5.6	Crystallisation trials.....	65
3.5.7	Data collection .....	65
<b>3.6</b>	<b>Initial maps of four point mutants of <i>Ec</i>-MnSOD.....</b>	<b>67</b>
3.6.1	General.....	67

## **4 Results ..... 69**

### **4.1 Structure of the azide-inhibited iron-substituted MnSOD from *E. coli* at 2.2 Å resolution.....69**

4.1.1 Merging and MR .....	69
4.1.2 Presence of azide ion at the active site.....	69
4.1.3 Refinement progress.....	71
4.1.4 Building solvent structure .....	72
4.1.5 Dimer structure .....	73
4.1.6 Geometric parameters.....	73
4.1.7 Building of active site, hydroxides and azide .....	74
4.1.8 Restraints.....	76
4.1.9 Structure of the active site of subunit A, with azide at 60% occupancy.....	77

### **4.2 MnSOD from *Deinococcus radiodurans* at 2.0 Å resolution ....78**

4.2.1 Quality of data .....	78
4.2.2 Molecular replacement and initial map interpretation.....	78
4.2.3 Geometric parameters of <i>Deino</i> -MnSOD.....	78
4.2.4 Active-site structures of <i>Deino</i> -MnSOD .....	80
4.2.5 Comparisons among the active sites of the four subunits .....	83
4.2.6 Description of the active site, angles and lengths of metal-binding ligands...	84

### **4.3 MnSOD from *Deinococcus radiodurans* with azide at the active site solved to 2.0 Å resolution at 116 K.....86**

4.3.1 Crystal .....	86
4.3.2 Merging, MR and initial maps .....	86
4.3.3 Refinement.....	86
4.3.4 Geometric parameters.....	92
4.3.5 Azide ion.....	92
4.3.6 Comparison of active sites between subunits .....	93
4.3.7 Description of the active site of the azide-bound form .....	95

### **4.4 Attempted high-temperature structure determination of *Deino*-MnSOD-N<sub>3</sub><sup>-</sup>.....96**

4.4.1 Results of attempted high-temperature data collection .....	96
4.4.2 Intermediate temperatures, below 0 °C.....	96

### **4.5 Point mutants of *Ec*-MnSOD .....**

4.5.1 Crystals .....	97
4.5.2 Quality of X-ray data, MR and initial maps .....	97

## **5 Critical evaluation of the structures of azide-inhibited MnSOD and FeSODs..... 99**

### **5.1 The structure of *Thermus*-MnSOD-N<sub>3</sub><sup>-</sup>.....99**

5.1.1 Structure solution and refinement protocols of <i>Thermus</i> -MnSOD-N <sub>3</sub> <sup>-</sup> .....	99
5.1.2 Summary of potential sources of error in <i>Thermus</i> -MnSOD-N <sub>3</sub> <sup>-</sup> .....	103
5.1.3 Resolution and coordinate errors .....	103
5.1.4 Interpretative bias .....	104

5.1.5	The use of two crystals .....	109
5.1.5.1	Saturated detector .....	109
5.1.5.2	Radiation damage .....	109
5.1.5.3	Missing data .....	110
5.1.5.4	Inherent difference in azide concentration between the crystals .....	111
5.1.5.5	Oxidation state .....	111
5.1.6	Data reduction .....	112
5.1.7	Possible sources of error within refinement .....	114
5.1.8	The refinement of water molecules, temperature factors and occupancy factors in <i>Thermus</i> -MnSOD-N <sub>3</sub> <sup>-</sup> .....	114
5.1.9	The lack of $R_{\text{free}}$ statistic .....	117
5.1.10	Problems with the starting model .....	118
<b>5.2</b>	<b><i>Thermus</i>-MnSOD .....</b>	<b>119</b>
5.2.1	The 4.4 Å resolution structure of <i>Thermus</i> -MnSOD .....	119
5.2.1.1	Original <i>Thermus</i> -MnSOD structural solution .....	119
5.2.2	The 2.4 Å resolution structure of <i>Thermus</i> -MnSOD .....	120
5.2.2.1	Phasing of medium-resolution <i>Thermus</i> -MnSOD structure .....	120
5.2.2.2	Refinement of medium resolution <i>Thermus</i> -MnSOD structure .....	121
5.2.3	The 1.8 Å resolution structure of <i>Thermus</i> -MnSOD .....	122
5.2.3.1	High-resolution structure of <i>Thermus</i> -MnSOD .....	122
5.2.3.2	Treatment of data .....	122
5.2.3.3	Discrepancies between published and deposited structures of <i>Thermus</i> -MnSOD .....	124
<b>5.3</b>	<b>Azide-inhibited FeSOD from <i>E. coli</i> .....</b>	<b>126</b>
5.3.1	Refining temperature factors and occupancy of water molecules .....	126
5.3.2	Refining alternate conformations of the active site .....	126
<b>5.4</b>	<b>Azide-inhibited FeSOD from <i>Pseudomonas ovalis</i> .....</b>	<b>127</b>
<b>5.5</b>	<b>Azide-inhibited cambialistic FeSOD from <i>Propionibacterium shermanii</i> .....</b>	<b>127</b>
<b>5.6</b>	<b>The inherent reliability of structures of azide-inhibited Fe/MnSODs .....</b>	<b>130</b>
5.6.1	<i>Ec</i> -FeSOD-N <sub>3</sub> <sup>-</sup> , <i>Psherm</i> -camb-FeSOD-N <sub>3</sub> <sup>-</sup> and Y174F- <i>Ec</i> -MnSOD-N <sub>3</sub> <sup>-</sup> .....	130
5.6.2	<i>Thermus</i> -MnSOD-N <sub>3</sub> <sup>-</sup> .....	130
5.6.3	<i>Pseudo</i> -FeSOD-N <sub>3</sub> <sup>-</sup> .....	131
<b>5.7</b>	<b>Convergent errors in azide-inhibited Cu/ZnSODs .....</b>	<b>131</b>
5.7.1	Quality of SOD structures .....	133
<b>6</b>	<b>Comparisons with other structures and discussion of results .....</b>	<b>135</b>
<b>6.1</b>	<b>Analysis and implications of the structure of <i>Ec</i>-Fe-MnSOD-N<sub>3</sub><sup>-</sup> at 2.2 Å resolution .....</b>	<b>135</b>
6.1.1	pH-dependent processes in <i>Ec</i> -Fe <sup>3+</sup> -MnSOD and <i>Ec</i> -Fe <sup>3+</sup> SOD .....	135
6.1.2	Structural features of <i>Ec</i> -Fe-MnSOD .....	138
6.1.3	Two active-site conformations imply communication across the dimer interface .....	141

6.1.4	Other differences between substituted and native forms.....	141
6.1.5	The mobile solvent-access funnel tyrosine.....	142
6.1.6	Structure of the active site of subunit B, without azide.....	144
6.1.7	Implications of the <i>Ec</i> -Fe-MnSOD-N <sub>3</sub> <sup>-</sup> structure.....	146
6.1.8	Orientation of azide in <i>Ec</i> -Fe-MnSOD-N <sub>3</sub> <sup>-</sup> and comparisons with other azide-inhibited Fe/MnSODs.....	146
6.1.9	How the structure of <i>Ec</i> -Fe-MnSOD-N <sub>3</sub> <sup>-</sup> relates to what is known.....	147
6.1.10	The solvent-access funnel tyrosine and hydrogen-bonding network.....	148
6.1.11	Thermochromic shifts.....	148
<b>6.2</b>	<b>Analysis and implications of the structure of <i>Deino</i>-MnSOD..</b>	<b>150</b>
6.2.1	Background.....	150
6.2.2	Other <i>Deino</i> -MnSOD structures.....	150
6.2.2.1	Structural comparison with Rec- <i>Deino</i> -Fe-MnSOD.....	151
6.2.3	Lack of product inhibition.....	152
6.2.4	Role of the catalytic cavity in by-product inhibition.....	153
6.2.5	Variation in a hydrophobic second-sphere residue across MnSODs that vary in product inhibition susceptibility.....	156
6.2.6	Asymmetrical proton environment at the dimer interface of <i>Deino</i> -MnSOD (and other Fe/MnSODs).....	157
<b>6.3</b>	<b>Analysis and implications of the azide-inhibited MnSOD from <i>Deinococcus radiodurans</i>.....</b>	<b>160</b>
6.3.1	Background: the use of azide as a substrate mimic.....	160
6.3.2	Implications of the <i>Deino</i> -MnSOD-N <sub>3</sub> <sup>-</sup> structure.....	161
6.3.3	Relevance of <i>Deino</i> -MnSOD-N <sub>3</sub> <sup>-</sup> to transition state.....	165
<b>6.4</b>	<b>Comparative effects of azide binding on hydrogen-bonding networks in Fe/MnSODs.....</b>	<b>165</b>
6.4.1	Effects of azide binding on hydrogen-bonding networks of FeSODs.....	166
6.4.2	The problem of evolving two azide-binding patterns from a unique common ancestor.....	171
6.4.3	Potential sources of error in <i>Deino</i> -MnSOD-N <sub>3</sub> <sup>-</sup> .....	171
6.4.4	Possible implications if the structure of <i>Thermus</i> -MnSOD-N <sub>3</sub> <sup>-</sup> is incorrect.....	172
6.4.5	Possible implications if the structure of <i>Deino</i> -MnSOD-N <sub>3</sub> <sup>-</sup> and <i>Thermus</i> -MnSOD-N <sub>3</sub> <sup>-</sup> are both correct.....	172
6.4.6	Differences in amino-acid sequence.....	172
6.4.7	pH differences between <i>Deino</i> -MnSOD-N <sub>3</sub> <sup>-</sup> and <i>Thermus</i> -MnSOD-N <sub>3</sub> <sup>-</sup> .....	174
6.4.8	Temperature of data collection.....	175
<b>6.5</b>	<b>Attempted ambient temperature X-ray diffraction data for <i>Deino</i>-MnSOD-N<sub>3</sub><sup>-</sup>.....</b>	<b>175</b>
<b>6.6</b>	<b>Mutants of <i>Ec</i>-MnSOD: preliminary crystallographic results</b>	<b>175</b>
6.6.1	S82T- <i>Ec</i> -MnSOD: preliminary results.....	176
6.6.2	L83M- <i>Ec</i> -MnSOD: preliminary results.....	176
6.6.3	L133V- <i>Ec</i> -MnSOD: preliminary results.....	176
6.6.4	M164L/L166V- <i>Ec</i> -MnSOD: preliminary results.....	176
<b>6.7</b>	<b>Discussion.....</b>	<b>177</b>
6.7.1	Entropic considerations of azide binding.....	177

6.7.2	Other variation between FeSODs and MnSODs interpreted as thermodynamic variation .....	180
6.7.2.1	Reduction potentials.....	180
6.7.2.2	Differences in solvent structure between azide-inhibited FeSODs and MnSODs .....	180
6.7.2.3	The altered pK of <i>Ec</i> -Fe-MnSOD.....	180
6.7.3	Second inhibition site .....	181
6.7.4	SODs with very low affinity for azide .....	181
6.7.5	Thermodynamic implications for native FeSODs and native MnSODs .....	182
6.7.6	Remote effects .....	182
6.7.6.1	Electrostatic .....	182
6.7.6.2	Tetramers.....	182
6.7.7	The role of mobile tyrosine .....	183
6.7.8	The role of conserved solvent-access funnel tyrosine in separating active site from solvent.....	183
6.7.9	Serious alterations to hydrogen-bonding network.....	184
6.7.10	Final thoughts and summing up .....	185

## **7 Inner-sphere proton-transfer mechanism for MnSODs ..... 187**

### **7.1 Linking structure and function of MnSODs .....187**

### **7.2 Known biochemistry.....187**

### **7.3 “Inner-sphere” scheme.....189**

### **7.4 First half-reaction: oxidation of superoxide by Mn<sup>3+</sup>SOD .....190**

7.4.1 Starting point: oxidised MnSOD..... 190

7.4.2 High-entropy binding of superoxide .....

7.4.3 Low-entropy bound state of superoxide .....

7.4.4 Water moves into the active site .....

7.4.5 Electron transfer to Mn<sup>3+</sup> and coupled proton uptake .....

7.4.6 End of the first half-reaction .....

### **7.5 Second half-reaction: reduction of superoxide by Mn<sup>2+</sup>SOD ..197**

7.5.1 Proposed second half-reaction: reduction of superoxide by Mn<sup>2+</sup> .....

7.5.2 Superoxide associates with metal ion .....

7.5.3 Water associates with superoxide ion .....

7.5.4 Electron transfer from Mn<sup>2+</sup> to superoxide and coupled proton transfer .....

7.5.5 The end of the second half-reaction .....

### **7.6 Implications of the inner-sphere mechanism .....203**

### **7.7 Differences between MnSODs and FeSODs.....204**

### **7.8 Evidence in support of inner-sphere proton transfer .....205**

### **7.9 Evidence against inner-sphere proton transfer .....207**

<b>8</b>	<b>An alternate, outer-sphere mechanism for proton transfer in MnSODs, that is independent of coordinated hydroxide .....</b>	<b>215</b>
8.1	“Outer-sphere” scheme .....	215
8.2	Sequence of events in the outer-sphere mechanism of proton transfer .....	216
8.2.1	Divergence from the inner-sphere mechanism .....	216
8.2.2	Water moves into the active site .....	217
8.2.3	First catalysis step in the outer-sphere mechanism.....	218
8.2.4	Outer-sphere mechanism, prior to association of second superoxide.....	219
8.2.5	Superoxide and water associate prior to second catalysis step .....	220
8.2.6	Second catalysis in the outer-sphere mechanism .....	222
8.2.7	Elimination of the peroxo species .....	224
8.3	Potential ambiguities in the outer-sphere mechanism .....	225
8.3.1	Location of the remote site of proton uptake .....	226
8.4	Implications of an outer-sphere mechanism .....	229
8.5	Potential differences between FeSODs and MnSODs in the outer-sphere mechanism.....	229
8.6	Evidence in support of the outer-sphere proton-transfer mechanism .....	230
8.7	Evidence against the outer-sphere proton transfer .....	231
<b>9</b>	<b>Conclusions and future directions .....</b>	<b>233</b>
9.1	Conclusions .....	233
9.2	Future directions and experiments.....	234
9.2.1	Specific to results presented in this thesis.....	234
9.2.2	The entire Fe/MnSOD field.....	234
<b>10</b>	<b>References.....</b>	<b>237</b>

## 0.4 List of figures

Figure 1-1. Apparatus used by Lavoisier in his early experiments with oxygen. ....	1
Figure 1-2. Wall-eyed stereo-diagrams of the tertiary structure of the three superoxide dismutase protein folds. ....	5
Figure 1-3. Comparison of the active sites of the three superoxide dismutase families. ....	15
Figure 2-1. Dimer interface of <i>Ec</i> -MnSOD showing contributions to the active site by the dimer partner. ....	22
Figure 2-2. Differences in tetramer formation amongst the Fe/MnSODs. ....	24
Figure 2-3. Wall-eyed stereo-diagram of the gating residues of the solvent-access funnel from <i>Ec</i> -MnSOD. ....	26
Figure 2-4. Wall-eyed stereo-diagram showing the solvent-accessible surface of <i>Ec</i> -FeSOD coloured by electrostatic potential. ....	27
Figure 2-5. Wall-eyed stereo-diagram of a conserved hydrogen-bonding motif that links the metal-coordinated solvent molecule to the tyrosine within the solvent-access channel. ....	31
Figure 2-6. Redox- and pH-dependent changes in active-site structure of FeSOD. ....	40
Figure 2-7. Temperature-, redox- and pH-dependent changes in active-site structure of MnSOD. ....	42
Figure 3-1. Strand overlap extension method used to generate point mutants. ....	60
Figure 3-2 Photograph of a SDS-PAGE showing protein samples before and after cation-exchange chromatography for four mutants of <i>Ec</i> -MnSOD. ....	63
Figure 3-3 Photograph of a SDS-PAGE showing fractions after anion-exchange chromatography for a S82T-MnSOD. ....	64
Figure 4-1. The improvement of omit maps during refinement from initial solution to final structure for the A subunit of <i>Ec</i> -Fe-MnSOD-N <sub>3</sub> <sup>-</sup> . ....	70
Figure 4-2. Stereo-image of the active site of subunit A of azide-bound <i>Ec</i> -Fe-MnSOD. ....	72
Figure 4-3. Testing the alternate azide-binding motif. ....	75
Figure 4-4. Active site of <i>Ec</i> -Fe-MnSOD-N <sub>3</sub> <sup>-</sup> for chain A. ....	76
Figure 4-5. Active site of <i>Ec</i> -Fe-MnSOD-N <sub>3</sub> <sup>-</sup> for chain B. ....	77
Figure 4-6. The MR solution of the <i>Deino</i> -MnSOD structure. ....	79
Figure 4-7. Electron-density maps from the molecular-replacement structural solution showing the quality of phases for <i>Deino</i> -MnSOD. ....	80

Figure 4-8. Active site of subunit A and nearby solvent-access funnel of <i>Deino</i> -MnSOD.....	81
Figure 4-9. Active site of subunit B and nearby solvent-access funnel of <i>Deino</i> -MnSOD.....	82
Figure 4-10. Active site of subunit C and nearby solvent-access funnel of <i>Deino</i> -MnSOD.....	82
Figure 4-11. Active site of subunit D and nearby solvent-access funnel of <i>Deino</i> -MnSOD.....	83
Figure 4-12. Overlay of the active sites of all four subunits of <i>Deino</i> -MnSOD. ....	84
Figure 4-13. Difference density peaks of the fifth and sixth ligands of the active-site Mn for <i>Deino</i> -MnSOD-N <sub>3</sub> <sup>-</sup> .....	87
Figure 4-14. Quality of phase information from the solution of <i>Deino</i> -MnSOD-N <sub>3</sub> <sup>-</sup> as shown in electron-density maps from early rounds of refinement. ....	88
Figure 4-15. Wall-eyed stereo-diagram showing electron-density maps at the active-site of the A subunit of <i>Deino</i> -MnSOD-N <sub>3</sub> <sup>-</sup> .....	90
Figure 4-16. Wall-eyed stereo-diagram showing electron-density maps at the active site of the B subunit of <i>Deino</i> -MnSOD-N <sub>3</sub> <sup>-</sup> .....	91
Figure 4-17. Wall-eyed stereo-diagram showing electron-density maps at the active site of the C subunit of <i>Deino</i> -MnSOD-N <sub>3</sub> <sup>-</sup> .....	91
Figure 4-18. Wall-eyed stereo-diagram showing electron-density maps at the active site of the D subunit of <i>Deino</i> -MnSOD-N <sub>3</sub> <sup>-</sup> .....	92
Figure 4-19. Hydrogen-bonding network that links the active site of <i>Deino</i> -MnSOD-N <sub>3</sub> <sup>-</sup> to the ordered solvent of the substrate-access funnel.....	93
Figure 5-1. The split-occupancy active site of azide-inhibited <i>Thermus</i> -MnSOD superposed onto the native structure.....	100
Figure 5-2. Flow diagram of the information used to solve the structure of <i>Thermus</i> -MnSOD-N <sub>3</sub> <sup>-</sup> .....	102
Figure 5-3 The active site of <i>Thermus</i> -MnSOD-N <sub>3</sub> <sup>-</sup> overlaid onto the electron-density maps for the four active sites of <i>Deino</i> -MnSOD-N <sub>3</sub> <sup>-</sup> showing a possible interpretative bias.....	105
Figure 5-4. Selected temperature factors within the active site of the A subunit of <i>Thermus</i> -MnSOD-N <sub>3</sub> <sup>-</sup> .....	107
Figure 5-5. Reproduction of the stereo-diagram showing peaks used to fit azide into <i>Thermus</i> -MnSOD-N <sub>3</sub> <sup>-</sup> (Lah <i>et al.</i> , 1995).....	108
Figure 5-6. Wall-eyed stereo-view of a potential steric clash of His146 with Trp126 in the submitted structure of <i>Psherm</i> -camb-FeSOD-N <sub>3</sub> <sup>-</sup> .....	128

Figure 5-7. Wall-eyed stereo-diagram of the modelled alternate rotamer of His146 that does not clash with Trp126, derived from the coordinates of <i>Psherm-camb-FeSOD-N<sub>3</sub><sup>-</sup></i> . .....	129
Figure 5-8. Structure of azide-bound Cu/ZnSODs, overlaid onto native structures, where the inhibitor displaces solvent molecules. ....	132
Figure 6-1. Proposed pH-dependent transitions with p <i>K</i> values in <i>Ec-Fe<sup>3+</sup>-MnSOD</i> . .	137
Figure 6-2. The active site of subunit A of <i>Ec-Fe-MnSOD</i> .....	138
Figure 6-3. The active site of subunit B of <i>Ec-Fe-MnSOD</i> . ....	139
Figure 6-4. The active site of subunit A of <i>Ec-FeSOD</i> .....	139
Figure 6-5. The active site of subunit A of <i>Ec-MnSOD</i> . ....	140
Figure 6-6. Resonance Lewis structures of the azide ion. ....	143
Figure 6-7. Overlay of the active site of the A subunits of <i>Ec-MnSOD</i> , <i>Ec-Fe-MnSOD</i> and <i>Ec-Fe-MnSOD-N<sub>3</sub><sup>-</sup></i> . ....	143
Figure 6-8. Overlay of the active site of the B subunits of <i>Ec-MnSOD</i> , <i>Ec-Fe-MnSOD</i> and <i>Ec-Fe-MnSOD-N<sub>3</sub><sup>-</sup></i> . ....	145
Figure 6-9. Wall-eyed stereo-image of an overlay of the active site of previously solved azido-Fe/MnSODs.....	147
Figure 6-10. Overlay of the active sites and nearby water molecules of WT- <i>Deino-MnSOD</i> and recombinant- <i>Deino-Fe-MnSOD</i> . ....	151
Figure 6-11. Walled-eyed stereo-images showing comparisons of the cavity behind the sixth ligand-binding site between <i>mito-MnSOD</i> (top), <i>Ec-MnSOD</i> (middle) and <i>Deino-MnSOD</i> (bottom). ....	154
Figure 6-12. Overlay of the region surrounding the solvent-access funnel tyrosine in <i>mito-MnSOD</i> , <i>Ec-MnSOD</i> and <i>Deino-MnSOD</i> . ....	155
Figure 6-13. A variable hydrophobic residue in the second-sphere of <i>mito-MnSOD</i> , <i>Ec-MnSOD</i> and <i>Deino-MnSOD</i> . ....	156
Figure 6-14. The hydrogen-bonding network at the dimer interface of <i>Deino-MnSOD</i> . .....	158
Figure 6-15. Asymmetric pattern of hydrogen atoms at the dimer interface of <i>Deino-MnSOD</i> .....	159
Figure 6-16. Wall-eyed stereo-image of the modelled binding of superoxide, based on the structure of <i>Deino-MnSOD-N<sub>3</sub><sup>-</sup></i> . ....	162
Figure 6-17. Overlay of the pertinent active-site structures of <i>Deino-MnSOD</i> and <i>Deino-MnSOD-N<sub>3</sub><sup>-</sup></i> , showing the movement of water into the active site upon azide binding. ....	163

Figure 6-18. Torsion angle that is drastically varied amongst different Fe/MnSODs solved with bound azide.....	167
Figure 6-19. System diagram part 1, azide-free Fe/MnSODs. ....	168
Figure 6-20. System diagram part 2, azide-bound Fe/MnSODs. ....	169
Figure 6-21. Alignment of the amino-acid sequences of <i>Thermus</i> -MnSOD and <i>Deino</i> -MnSOD, performed by ClustalW (version 2.0.5). ....	174
Figure 6-22. Reaction-coordinate diagrams of MnSOD, FeSOD, and Fe-MnSOD in the presence of azide at high and low temperatures. ....	179
Figure 7-1. Unsymmetrical distribution of electrons within the superoxide molecule near the active-site Mn <sup>3+</sup> . ....	188
Figure 7-2. Starting state for the first half-reaction of the inner-sphere mechanism. ...	191
Figure 7-3. The arrival of superoxide at the active site for the first half-reaction of the inner-sphere mechanism. ....	193
Figure 7-4. Rearrangement of hydrogen bonding after coordination of superoxide in the first half-reaction of the inner-sphere mechanism.....	194
Figure 7-5. Arrival and hydrogen bonding of water to superoxide in the first half-reaction of the inner-sphere mechanism. ....	195
Figure 7-6. Coupled proton and electron transfer in the first half-reaction of the inner-sphere mechanism. ....	196
Figure 7-7. Departure of dioxygen and water from the active site in the first half-reaction of the inner-sphere mechanism. ....	197
Figure 7-8. Starting state for the second half-reaction of the inner-sphere mechanism. ....	198
Figure 7-9. Arrival of superoxide at the active site in the second half-reaction of the inner-sphere mechanism. ....	199
Figure 7-10. Arrival and binding of water to the superoxide ion for the second half-reaction of the inner-sphere mechanism. ....	200
Figure 7-11. Coupled electron and proton transfer in the second half-reaction of the inner-sphere mechanism. ....	201
Figure 7-12. Departure of hydrogen peroxide and water in the second half-reaction of the inner-sphere mechanism. ....	202
Figure 7-13. Wall-eyed stereo-image, looking down the solvent-access funnel, showing the potential steric clashes if the solvent-derived molecule is an hydroxide ion. ....	209
Figure 7-14. Wall-eyed stereo-image, looking down the solvent-access funnel, showing the potential steric clashes if the solvent-derived molecule is a water. ....	209

Figure 7-15. Wall-eyed stereo-image, looking down the bond between active-site Mn and the solvent-derived molecule, here modelled as an hydroxide ion.....	211
Figure 7-16. Wall-eyed stereo-image, looking down the bond between active-site Mn and the solvent-derived molecule, here modelled as a water.....	211
Figure 7-17. Ultra-high-resolution electron-density maps of the active-site of the A subunit of the oxidised form of Y174F- <i>Ec</i> -MnSOD where positive peaks in difference maps may be hydrogen atoms.....	212
Figure 7-18. Ultra-high-resolution electron-density maps of the active-site of the A subunit of the reduced form of Y174F- <i>Ec</i> -MnSOD where positive peaks in difference maps may be hydrogen atoms.....	213
Figure 8-1. Binding of superoxide in the low-entropy state for the first half-reaction of the outer-sphere mechanism. ....	217
Figure 8-2. Arrival and binding of water to the superoxide ion for the first half-reaction of the outer-sphere mechanism. ....	218
Figure 8-3. Coupled electron and proton transfer in the first half-reaction of the outer-sphere mechanism. ....	219
Figure 8-4. Starting state for the second half-reaction of the outer-sphere mechanism. ....	220
Figure 8-5. Binding of water and superoxide in the second half-reaction of the outer-sphere mechanism. ....	221
Figure 8-6. Ordered water linking the superoxide ion to the remote site of proton uptake. ....	222
Figure 8-7. Coupled electron and proton transfer in the second half-reaction of the outer-sphere mechanism. ....	223
Figure 8-8. Arrangement of protons after the second catalysis step of the outer-sphere mechanism.....	224
Figure 8-9. Final protonation of the peroxo species in the second half-reaction of the outer-sphere mechanism. ....	225
Figure 8-10. Reduction/oxidation linked changes in selected side chains of Y174F- <i>Ec</i> -MnSOD.....	227
Figure 8-11. The active sites of the dimer of <i>Deino</i> -MnSOD and the waters that line the dimer interface.....	228

Colour images occur on the following pages

5,15,22,24,26,27,31,70,72,75,76,77,79,80,81,82,82,83,84,87,88,90,91,91,92,93,100,105

,

107,128,129,132,138,139,139,140,143,145,147,151,154,155,156,158,159,162,163,209,

209,211,211,212,213,227,228.

## 0.5 List of equations

Equation 1.....	16
Equation 2.....	16
Equation 3.....	108
Equation 4.....	109
Equation 5.....	109
Equation 6.....	113
Equation 7.....	117
Equation 8.....	152
Equation 9.....	152
Equation 10.....	152
Equation 11.....	152
Equation 12.....	153
Equation 13.....	177
Equation 14.....	180
Equation 15.....	180
Equation 16.....	187
Equation 17.....	187
Equation 18.....	187
Equation 19.....	189
Equation 20.....	189
Equation 21.....	189
Equation 22.....	190
Equation 23.....	190
Equation 24.....	190
Equation 25.....	190
Equation 26.....	190

Equation 27.....	215
Equation 28.....	215
Equation 29.....	215
Equation 30.....	216
Equation 31.....	216
Equation 32.....	216

## 0.6 List of tables

Table 1. Data merging and refinement statistics for <i>Ec</i> -Fe-MnSOD and <i>Ec</i> -Fe-MnSOD-N <sub>3</sub> <sup>-</sup> .....	50
Table 2. Data merging and refinement statistics for <i>Deino</i> -MnSOD and <i>Deino</i> -MnSOD-N <sub>3</sub> <sup>-</sup> .....	54
Table 3. PCR primers used for mutation .....	61
Table 4. Components of crystal trial used to generate a gradient in the precipitant PEG 6000. ....	65
Table 5. Data collection and initial refinement statistics for four point mutants of <i>Ec</i> -MnSOD.....	66
Table 6. Bond angles of the active-site Mn and metal-ligating atoms of <i>Deino</i> -MnSOD. ....	85
Table 7. Bond lengths between the active-site Mn and metal-ligating atoms of <i>Deino</i> -MnSOD.....	85
Table 8. Bond angles between the active-site Mn and the metal-ligating atoms of <i>Deino</i> -MnSOD-N <sub>3</sub> <sup>-</sup> .....	95
Table 9. Bond lengths between the active-site Mn and metal-ligating atoms of <i>Deino</i> -MnSOD-N <sub>3</sub> <sup>-</sup> .....	96
Table 10. The distribution of occupancy and temperature factors of ordered solvent within <i>Thermus</i> -MnSOD-N <sub>3</sub> <sup>-</sup> .....	115
Table 11. The distribution of occupancy and temperature factors of ordered solvent within <i>Ec</i> -FeSOD-N <sub>3</sub> <sup>-</sup> .....	126
Table 12. Summary of known <i>Deino</i> -MnSOD structures within the PDB.....	150
Table 13. Effect of azide binding on bond angles at the active-site manganese ion.....	164
Table 14. Effect of azide binding on bond lengths at the active-site Mn. ....	164
Table 15. Bond distances, bond angles and selected torsion angle of metal-ligating atoms in azide-inhibited Fe/MnSODs. ....	170

## 0.7 Abbreviations

$\alpha$ helix	secondary structure element of proteins
ATP	adenosine-5'-triphosphate
$\beta$ -sheet	secondary structure element of proteins
CD	circular dichroism
DNA	2'-deoxyribonucleic acid
$E^{\circ}$	standard reduction potential at pH 7
EPR	electron paramagnetic resonance
HFEP	high-magnetic field electron paramagnetic resonance
HPLC	high pressure liquid chromatography
K	kelvin, temperature scale
$k_{\text{cat}}$	the maximum number of enzymatic reactions catalysed per second
$K_m$	Michaelis constant, approximate substrate concentration, where enzyme activity is half the maximum
L	Litre, measure of volume
LB	Luria broth, media for bacterial growth
M	moles/litre, a measure of concentration
MCD	magnetic circular dichroism
MR	molecular replacement
MIR	multiple isomorphous replacement
mRNA	messenger RNA
mV	millivolt, a thousandth of a volt

NAD(P)H	nicotinamide adenine dinucleotide (phosphate) –reduced form
NCS	non-crystallographic symmetry
NMR	nuclear magnetic resonance
PCR	polymerase chain reaction
PDB	protein data bank
pH	activity of the hydrogen ion, measure of acidity, where $\text{pH} = -\log a_{\text{H}^+}$
p <i>K</i>	disassociation constant of a proton or a hydroxide, defined as $\text{p}K = -\log K$
redox	reduction/oxidation
<i>R</i> <sub>free</sub>	set of reflections, excluded from refinement and (electron) density calculations
RMS	root-mean-square, measure of the magnitude of a varying quantity. As RMS deviation, measure of scatter of values about a target value. Relevant to geometric parameters in protein structures.
RNA	ribonucleic acid
ROS	reactive oxygen species, including O <sub>2</sub> <sup>-</sup> , H <sub>2</sub> O <sub>2</sub> , O <sub>2</sub> NO <sup>-</sup> (peroxynitrate), OCl <sup>-</sup> (hypochlorite)
RPM	revolutions per minute
SIR	single isomorphous replacement
SOD	superoxide dismutase
SD	standard deviation
TLS	translation-libration-screw

$\mu\text{L}$	microlitre, measure of volume
UV	ultra violet
V	volt, potential difference across a conductor

## 0.8 Naming conventions of superoxide dismutases.

Throughout the literature concerning superoxide dismutases different naming conventions have been used for both genes and proteins. Some known names are Cu,ZnSOD, Cu-Zn superoxide dismutase, FeSOD, MnSOD, SOD, SOD-1, SOD-2, SOD-3, SOD-4, SODF, SODS, copper-zinc superoxide dismutase, cuprein, cytocuprein, erythrocuprein, ferrisuperoxide dismutase, hemocuprein, hepatocuprein, superoxidase dismutase, superoxide dismutase I, superoxide dismutase II, *et cetera*.

The most common abbreviations of superoxide dismutase are “SOD” pertaining to protein and “sod” for dealing with genes, but some have used “SD”. Superoxide dismutase activity has been detected in a number of polypeptides and subsequently potential superoxide dismutase activity has been inferred for many genes. Many organisms have multiple superoxide dismutases and a variety of naming schemes have been used.

sodA, sodB, sodC...	alphabetically based.
sod1, sod2, sod3...	numerically based.
<i>sodA, sod1..</i>	italicised to indicate gene.
sodM, sodF, sodN...	where the letter refers to the obligate metal cofactor Mn, Fe, Ni.

In this thesis a functional and hierarchical nomenclature will be used to describe the enzyme function, the obligate metal cofactor, oxidation state, the species of origin, inhibitors and mutation. Throughout this work “SOD” will be used as an abbreviation for superoxide dismutase. Members will be identified first by the element symbol, then abbreviation, for example “NiSOD” for a nickel-specific superoxide dismutase. Hierarchical naming systems have been used in several papers: the system used here is an extension, albeit with minor modifications, of that used by Vance and Miller (Vance & Miller, 1998b).

1. There are at present three major families of superoxide dismutases: nickel dependent (NiSOD), those which require both copper and zinc (Cu/ZnSOD), and the third family that are active with either manganese (MnSOD) or iron

(FeSOD). The abbreviations of “MnSOD” and “FeSOD” are treated as words beginning with vowels; e.g. “FeSOD” should be pronounced “eff-ee-sod” rather than as “i-arn-sod” and should be prefixed by the indefinite object, “an”, rather than “a”.

2. If it is unknown or ambiguous whether a superoxide dismutase is active with manganese or iron it is designated “Fe/MnSOD”. There are some members that have significant activity with both iron and manganese and these are commonly termed “cambialistic” These are referred to as “camb-Fe/MnSOD”, and hence the manganese-only form of a cambialistic enzyme would be “camb-MnSOD”.

3. If the redox state of the active-site metal is known it is denoted as a superscript of the elemental symbol. For example, “camb-Fe<sup>3+</sup>SOD” and “camb-Fe<sup>2+</sup>SOD” denote two different oxidation states of the iron in a cambialistic enzyme.

4. It is possible to generate superoxide dismutases with incorrect metal ions substituted for the preferred metals. The preferred metal is indicated immediately adjacent to the SOD expression, preceded by the metal that has been substituted, separated by a hyphen. For example, “Mn-FeSOD” represents an iron superoxide dismutase in which active-site iron is replaced with manganese.

5. By default the enzyme is assumed to have the native sequence. If increased clarity is required, then the prefix “WT” will be used as an abbreviation for “wild type”. If the protein has a point mutation it will be indicated by a prefix. The prefix will be the single letter code of the native sequence, followed by the residue number and the single letter code of the mutant. For example “Y34F-MnSOD” represents a mutation of a tyrosine to a phenylalanine at position 34 in an MnSOD. This is in contrast to the non-mutated native or “WT-MnSOD”.

6. The species of origin is indicated by an italicised expression between the indication of mutation and the metal designation. The basis of the italicised expression may either be the common or the scientific name. For example, “Y34F-*Ec*-MnSOD” and “Y34F-*mito*-MnSOD” represent the same point

mutation of the *Escherichia coli* and the human mitochondrial manganese superoxide dismutases respectively.

7. Superoxide dismutases interact with a number of small-molecule inhibitors to form stable complexes; this is indicated by the chemical name (and charge) of the inhibitor, written after the “SOD” expression. The azide-inhibited form of the cattle Cu/Zn superoxide dismutase would be indicated as “*bovine-Cu/ZnSOD-N<sub>3</sub><sup>-</sup>*”.

8. Other experimental techniques and variables can be included into this naming convention. These will be introduced after any description of inhibitors. For example “RT” is used to abbreviate for room temperature and “110 K” for an experiment at cryo-conditions of 110 K. For example, there exist spectral studies for Y34F-*Ec*-MnSOD-N<sub>3</sub><sup>-</sup> at ambient and cryogenic conditions designated “Y34F-*Ec*-MnSOD-N<sub>3</sub><sup>-</sup>-RT” and “Y34F-*Ec*-MnSOD-N<sub>3</sub><sup>-</sup>-110 K” respectively.

9. This nomenclature lends itself to the identification of individual atoms within a structure. This follows the hierarchy of protein name, underscore, chain identifier (italicised), underscore, one-letter amino acid code, residue number, underscore, and atom name. Atom names are capitalised forms, following the naming conventions of the protein data bank (Berman *et al.*, 2000). This makes distinguishing atoms that are closely located spatially unambiguous. The expressions “*Ec*-MnSOD\_A\_D146\_OD1” and “*Ec*-MnSOD\_A\_D146\_OD2” distinguishes between two atoms of the same amino-acid side chain. If there is a known PDB code for a protein, then this can be substituted for the protein name, for example “1VEW\_A\_D146\_OD1”.

10. If an atom or side chain in a crystal structure has split or multiple conformations then this will be indicated by a subscript after the atom name. For example, individual atoms within the two conformations of lysine 29 in the A chain of Y174F-*Ec*-MnSOD are described as “1IXB\_A\_K29\_NZ<sub>A</sub>” and “1IXB\_A\_K29\_NZ<sub>B</sub>”

11. The naming of water molecules will follow the hierarchy of protein name, underscore, an italicised chain number (if present), underscore, “WAT” followed by the number of the water, for example 1EN5\_WAT72.

The naming and abbreviation of amino acids generally follow IUPAC conventions for the use of trivial names, three-letter system and one-letter system (Cornish-Bowden, 1984). The naming and use of elements and chemicals will follow IUPAC conventions, but some trivial names will also be used.